



HAL
open science

Evaluation of antibacterial textile covered by layer-by-layer coating and loaded with chlorhexidine for wound dressing application

Francois Aubert-Viard, Alejandra Mogrovejo Valdivia, Nicolas Tabary, Mickael Maton, Feng Chai, Christel Neut, Bernard Martel, Nicolas Blanchemain

► To cite this version:

Francois Aubert-Viard, Alejandra Mogrovejo Valdivia, Nicolas Tabary, Mickael Maton, Feng Chai, et al.. Evaluation of antibacterial textile covered by layer-by-layer coating and loaded with chlorhexidine for wound dressing application. *Materials Science and Engineering: C*, 2019, *Materials Science and Engineering: C*, 100, pp.554-563. 10.1016/j.msec.2019.03.044 . hal-02114423

HAL Id: hal-02114423

<https://hal.univ-lille.fr/hal-02114423>

Submitted on 22 Oct 2021

HAL is a multi-disciplinary open access archive for the deposit and dissemination of scientific research documents, whether they are published or not. The documents may come from teaching and research institutions in France or abroad, or from public or private research centers.

L'archive ouverte pluridisciplinaire **HAL**, est destinée au dépôt et à la diffusion de documents scientifiques de niveau recherche, publiés ou non, émanant des établissements d'enseignement et de recherche français ou étrangers, des laboratoires publics ou privés.



Distributed under a Creative Commons Attribution - NonCommercial 4.0 International License

1 **Evaluation of antibacterial textile covered by Layer-by-Layer coating and**
2 **loaded with Chlorhexidine for wound dressing application**

3

4 François Aubert-Viard^{a,b}, Alejandra Mogrovejo-Valdivia^a, Nicolas Tabary^b, Mickael Maton^a,
5 Feng Chai^a, Christel Neut^c, Bernard Martel^b, Nicolas Blanchemain^{a*}

6

7 ^a Univ. Lille, INSERM, CHU Lille, U1008 - Controlled Drug Delivery Systems and
8 Biomaterials, F-59000 Lille, France

9 ^b Univ. Lille, CNRS UMR8207, UMET - Unité Matériaux et Transformations, F-59655
10 Villeneuve D'Ascq, France

11 ^c Univ. Lille, INSERM, CHU Lille, U995- LIRIC - Lille Inflammation Research International
12 Center, F-59000 Lille, France

13

14 * Corresponding author. Dr. Nicolas Blanchemain

15 E-mail : nicolas.blanchemain@univ-lille2.fr

16 Address: INSERM U1008, Controlled Drug Delivery Systems
17 and Biomaterials, College of Pharmacy, University Lille 2,
18 59006 Lille, France

19 Tel.: +33 320 62 69 75

20 Fax: +33 320 62 68 54

21 **Abstract**

22 The aim of this work is to design a wound dressing able to release chlorhexidine (CHX) as
23 antiseptic agent, ensuring long-lasting antibacterial efficacy during the healing. The textile
24 nonwoven (polyethylene terephthalate) (PET) of the dressing was first modified by chitosan
25 (CHT) crosslinked with genipin (Gpn). Parameters such as the concentration of reagents (Gpn
26 and CHT) but also the crosslinking time and the working temperature were optimized to reach
27 the maximal positive charges surface density. This support was then treated by the layer-by-
28 layer (LbL) deposition of a multilayer system composed of methyl-beta-cyclodextrin polymer
29 (PCD) (anionic) and CHT (cationic). After a thermal treatment to stabilize the LbL film, the
30 textiles were loaded with CHX as antiseptic agent. The influence of the thermal treatment i)
31 on the cytocompatibility, ii) on the degradation of the multilayer system, iii) on CHX sorption
32 and release profiles and iv) on the antibacterial activity of the loaded textiles was studied.

33

34 **Keywords**

35 Antibacterial textile, Chitosan, Genipin, cytocompatibility, Cyclodextrin, Chlorhexidine,
36 Layer-by-Layer

37 1. Introduction

38 Skin is the largest (1.2 to 2.3 m²) and heaviest (10 to 16% of the total body mass) organ of the
39 human body and is structured in three layers: the epidermis, the dermis and the hypodermis
40 from the most superficial to the deepest. This structure provides to the skin several functions:
41 sensitivity (temperature, touch of solids, liquids), thermal regulation of the body and
42 protective barrier against physical, chemical and foreign microorganisms aggressions [1].
43 Various factors may damage this protection such as wounds, bedsores or scars that pave the
44 way for pathogens and subsequent complications.

45 Indeed, infections provoke tissues necrosis, subsequently delay the healing process and extend
46 the healing period with dramatic consequences for the patient. The most frequent harmful
47 germ is *Staphylococcus aureus* (24 to 50%) [2–4]. Nevertheless, in most of cases the infection
48 is poly-microbial with the presence of other bacterial strains such as *Staphylococcus*
49 *epidermidis*, *Escherichia coli* or *Pseudomonas aeruginosa* [5–10]. Infected wounds request
50 the use of antibacterial dressings to eradicate bacterial colonization and eliminate biofilm in
51 order to allow the beginning of healing process in a second time. As necrotic tissues are
52 poorly irrigated, local treatments give better results than systemic administration. In the state-
53 of-the art, antibacterial dressings present biocide functionality through contact killing
54 provided by specific chemical groups such as alkyl ammonium groups [11] or through the
55 release of antiseptic agents such as chlorhexidine (CHX), triclosan, silver salts or
56 nanoparticles [12,13].

57 Chitosan (CHT) is a polymer of choice for use in wound dressings due to its biocompatible
58 [14,15] biodegradable, bacteriostatic, mucoadhesive and hemostatic properties [16–20]. CHT
59 is a natural polysaccharide obtained from deacetylation of chitin extracted from crustacean
60 shells and composed by D-2-deoxy-2-acetyl-glucosamine and D-2-deoxy-glucosamine units
61 linked by β (1→4) binding. The presence of basic amino functions (-NH₂) confers to CHT a

62 polycationic character in acidic conditions due to their transformation in ammonium groups (-
63 NH_3^+). Besides, CHT benefits from the high chemical reactivity of its amino groups toward
64 crosslinking reactions by using di-functional molecules such as glutaraldehyde, polyethylene
65 glycol epoxy polymer [21–23] or various compounds like polycarboxylic acids[24] and in
66 particular genipin (**Gpn**) used in the present study [15,25]. As a matter of fact, it is well
67 known that most of the crosslinking agents and especially di-aldehydes are toxic, making
68 them unsuitable for biomedical applications. On contrary, **Gpn** extracted from fruits of
69 *Gardenia jasminoides Ellis* is commonly used in pharmaceutical or food industry as pigment
70 precursor for food dyeing. Besides, **Gpn** readily reacts with primary amino groups of CHT
71 and proteins leading to their crosslinking [26–28]. This compound is recognized to be less
72 cytotoxic than most of crosslinking agents, especially glutaraldehyde [15] and is therefore
73 acceptable for biomaterials application.

74 Moreover, the crosslinking reaction by **Gpn** occurs in mild conditions *i.e.* at room
75 temperature, which are favourable to highly heat-sensitive compounds such as proteins or
76 substrates such as textiles. Thus, Liu & Huang have developed a bilayer dressing based on soy
77 protein and CHT film crosslinked by **Gpn** to improve epithelialization and repair of injuries
78 [28]. More recently, Martin *et al* reported coating of a textile support by a polyelectrolyte
79 multilayer (PEM) system obtained from the self-assembly of CHT and an anionic
80 cyclodextrin polymer (**PCD**) bearing carboxylate groups [29,30]. The cohesion of such
81 nanostructured system was directed by the formation of polyelectrolyte complexes (PEC)
82 formed between CHT and **PCD** and its stability in aqueous media depended on the pH and on
83 ionic strength of the medium [31].

84 The incorporation or immobilization of antibacterial agents (methylene blue, **CHX**, metallic
85 ions) on wound dressing is used to prevent wound infections [32]. **CHX** is a biguanide
86 compound widely used for the local bucco-pharyngeal, cutaneous antiseptics with a broad-

87 spectrum activity and can be used in association with other antibacterial compounds such as
88 benzalkonium chloride in particular in Biseptine[®] principally used for cutaneous application.
89 The association of CHX with other compounds like iodine has also been reported to improve
90 the antibacterial effect of the CHX (synergic effect) [33].

91 This study reports the elaboration of an antibacterial textile coated by a first layer of CHT
92 immobilized by crosslinking with Gpn, onto which a polyelectrolyte multilayer (PEM) film
93 was built up, consisting of the self-assembled layers of anionic PCD and cationic CHT. The
94 antibacterial activity of the modified textiles was determined by release-killing effect after
95 loading the PEM system with CHX. In our concept, the PCD is expected not only to provide
96 enhanced reservoir and sustained release properties to the PEM system thanks to the CHX-
97 cyclodextrin (CD) inclusion complexes formation and to its slow dissociation.

98 This paper reports the impact of sample preparation conditions on the first crosslinked CHT
99 layer with Gpn, which was necessary to provide cationic sites firmly anchored to the neutral
100 polyester fibres, and then the PEM build-up construction will be investigated. The *in vitro*
101 CHX kinetic of release is studied in parallel with the *in vitro* antibacterial tests on *S. aureus*.
102 As this support is destined for contact with superficial and deep tissues composing the skin,
103 an evaluation of the cytocompatibility of functionalized textiles was also conducted.

104 2. Materials and methods

105 2.1. Materials and reagents

106 The textile support used was a non-woven polyethylene terephthalate (PET, NSN 365)
107 provided by PGI-Nordlys (Bailleul, France). The density of PET was 76 g/cm² and the
108 thickness 0.24 mm. Before chemical modification, the textiles were thoroughly washed by
109 three successive cycles of soxhlet extraction with isopropanol and distilled water. **PET was**
110 **chosen for its biocompatibility, low price and wide use in commercially available wound**
111 **dressings.**

112 **Gpn**, acetic acid, CHT and Phosphate Buffered Saline (PBS) were purchased from Sigma
113 Aldrich (Saint Louis, USA). CHT was a low molecular weight grade (batch N° SLBG1673V,
114 190 kDa, viscosity: 20-300, in 1%v/v acetic acid) with a degree **of deacylation (DD) of 80%**
115 **+/-5% (according to supplier) and the calculated NH₂ content was 5.0 +/-0.25 mmol/g.** PBS
116 solution was prepared by dissolving one tablet in 200 mL of ultrapure water (Pure Lab Flex
117 Elga, Veolia). The final concentration was 0.01 M phosphate buffer, 0.0027 M potassium
118 chloride and 0.137 M sodium chloride (pH 7.4 at 25 °C). **CHX** was purchased from INRESA
119 (Bartenheim, France)

120 2-O-Methyl β -cyclodextrins (Me β CD Crysmeb®, DS = 0.50) was purchased from Roquette
121 (Lestrem, France). Anionic water-soluble **PCD** was synthesized according to a method
122 patented by Weltrowski et al. [34]. Citric acid as crosslinking agent, sodium hypophosphite as
123 catalyst and Me β CD in respective weight ratio 10/3/10 (g in 100 mL) were dissolved in water.
124 After water removal using a rotative evaporator, the resulting solid mixture was then cured at
125 140°C during 30 min under vacuum. Water was then added and the resulting suspension was
126 filtered, and dialyzed during 72 h in water using 6–8 kDa membranes (SPECTRAPOR 1,
127 Spectrumlabs). Finally, the water-soluble anionic CD polymer (**PCD**) was recovered after
128 freeze drying. The weight composition of **PCD**, was 74 wt.% in Me β CD moieties (determined

129 by ¹H NMR) and the calculated carboxylate groups content was 2.7 +/-0.3 mmol/g. The
130 molecular mass in number (Mn) of PCD was 8 000 g/mol, measured by size exclusion
131 chromatography SEC) in water equipped with a light scattering detector.

132 2.2. Chitosan fixation on PET with genipin (PET-CHT)

133 CHT-1% (w/v) and CHT-2.5% (w/v) were obtained by dissolving CHT in 1% (v/v) acetic
134 acid. Gpn was solubilised in distilled water to obtain final concentrations of 0.01; 0.05; 0.1
135 and 0.5% (w/v) after mixing with CHT solution. The virgin PET textile (5*5cm) was weighed
136 on a precision balance (+/-10⁻⁴g, Kern, Balingen, Germany) (initial weight (w_i)), impregnated
137 in the different CHT/Gpn solutions and roll-padded (Roaches, England). Samples were placed
138 in an incubator at 25°C under wet atmosphere (RH-100%) for 48 hours, where crosslinking
139 reaction occurred. The textiles were finally washed in acetic acid (1% (v/v), 20 min) and
140 ultrapure water (20 min, 2 times) under sonication to remove the unreacted CHT and Gpn,
141 dried at 90°C for 1 hour and weighed (w_f). The degree of functionalization was calculated by
142 the weight gain:

143 Eq. 1:
$$\text{Weight gain (\%)} = \frac{w_f - w_i}{w_i} \times 100$$

144 where w_i and w_f represent the weight of the nonwoven PET samples before and after their
145 modification with CHT-Gpn (named PET-CHT), respectively.

146 2.3. Layer-by-layer coating (PET-CHT-PEMn).

147 The multilayer assembly was built using the dip-coating method as previously reported
148 [29,30] and schematized in Figure 1. Samples (5 × 5 cm) were cut off from PET-CHT
149 samples (described in the previous section) and alternately dipped during 15 min in the PCD
150 solution (0.3% (w/v) in ultrapure water) and in the CHT solution (0.5% (w/v)) in acetic acid
151 1% (v/v) with intermediate drying and rinsing steps according at room temperature under

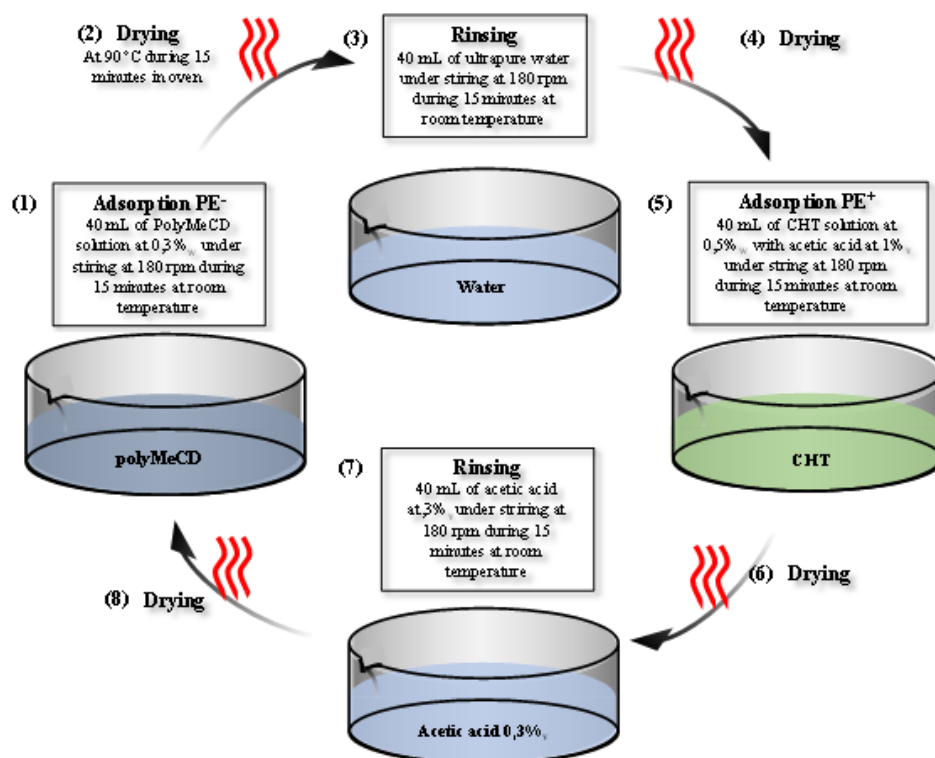
152 stirring (180 rpm). The weight gain after each further polyelectrolyte layer was determined
153 following this equation.

154 Eq. 2:
$$\text{Weight gain (\%)} = \frac{W_{\text{dip-coating}} - W_i}{W_i} \times 100$$

155 Where w_i is the weight of the virgin PET sample and $w_{\text{dip-coating}}$ is the sample weight after its
156 modification by CHT-Gpn then followed by n dip-coating cycles.

157

158 The first self-assembled PCD layer adsorbed onto the CHT-Gpn primer layer (layer #1)
159 grafted on the textile was labelled layer #2, while the following self-assembled CHT layer
160 was labelled layer #3. So CHT layers of the system were numbered with odd values and
161 samples terminated with 11 layers (PEM11), 15 layers (PEM15) and 21 layers (PEM21) were
162 used as test samples. Finally, the modified textiles were cured at 140°C for 105 min to
163 stabilize the PEM. Sample were named PET-CHT-PEM n , where n is the number of layer.



164

165 *Figure 1. Schematization of the dip-coating process to build-up the multilayer system.*

166 2.4. Textiles characterization

167 2.4.1. Acid orange titration

168 The titration of free amino group content on the textile was realized by the method
169 described by Aubert *et al* [24]. The samples (disks of 11 mm diameter) were dipped in an
170 orange acid (OA) solution at 2.5×10^{-2} M, pH3 at room temperature overnight under stirring
171 (300 rpm). A calibration curve is realized preliminary with OA solution at 0.4 mM in pure
172 water.

173 The amount of amino functions is calculated as follows:

174 Eq. 3:

$$\text{NH}_2, \text{ mmol/g} = \frac{\text{Absorbance} \times \text{volume (L)}}{\text{Slope (L.mol}^{-1}.\text{cm}^{-1})} / \text{weight (g)}$$

175 Where “slope” is the molar extinction coefficient measured from the calibration (value =
176 0,014 L.mol⁻¹.cm⁻¹)

177 2.4.2. Scanning Electron Microscopy (SEM)

178 The SEM investigations of functionalized textiles were carried out on a Hitachi S-4700 SEM
179 FEG (Field Emission Gun) operating with an acceleration voltage of 5–25 kV, after carbon
180 metallization.

181 2.4.3. Degradation studies

182 The kinetics of degradation of the PEM system was performed before and after heat
183 post-treatment at 140°C. The samples (Ø 11 mm, n = 3) are weighed (w_i) and then immersed
184 in 10 ml of a PBS solution (37°C, 80 rpm). At regular time intervals, the samples were rinsed
185 twice with 2 mL of ultrapure water to remove the salts adsorbed on textiles and dried at 90°C
186 in a ventilated oven for 15 minutes. Textiles were finally weighed (w_d) and put back in fresh

187 PBS. The results were calculated as a percentage of the remaining mass as a function of time
188 as follow:

189 Eq. 4:

$$\text{Remaining Mass (\%)} = \frac{w_d}{w_i} \times 100$$

190 2.4.4. *In vitro biological evaluation - Cell viability*

191 The human embryonic epithelial cell line (L132) were selected for testing the
192 cytocompatibility of CHT functionalized textiles due to their relevance to target clinical
193 application (skin care) and its good reproducibility. Cells were cultured in modified minimum
194 essential medium (MEM, Gibco[®], LifeTechnology) supplemented with 10% foetal calf serum
195 (FCS, Gibco[®], LifeTechnology).

196 After disinfection by dipping in absolute alcohol and drying at 37°C overnight, the disk
197 samples (PET, PET-CHT, PET-CHT-PEMn) were placed in the bottom of 24-well plates
198 (Costar, Starlab). Viton rings (Radiospare) were inserted into the wells to prevent the floating
199 of samples, and subsequently avoid cells growing beneath the test samples. Cells were gently
200 seeded at the density of 3500 cells cm⁻² in each well, and the wells with no sample disk but
201 only cell suspension served as controls, tissue culture polystyrenes (TCPS). The growth
202 periods for the cell proliferation and cell vitality tests were 3 and 6 days without renewal of
203 the medium.

204 3 and 6 days after the cell seeding, the culture medium was removed from each well and
205 500 µL of culture medium diluted fluorescent dye (AlamarBlue[®], Interchim) was deposited in
206 each well. After incubation at 37°C for 2 hours, the reacted dye solutions were transferred
207 into 96-well plates (VWR International) and the non-toxic fluorescence was measured by
208 fluorimeter (Twinkle LB970TM Berthold) at 560 nm. Data were expressed as the mean

209 percentage \pm SD of six separate experiments with respect to the control (Tissue Culture
210 PolyStyrene, TCPS – 100 %).

211 **2.5. Textiles loading with chlorhexidine**

212 **2.5.1. CHX quantification**

213 High-Performance Liquid Chromatography (HPLC) coupled to UV detection (HPLC-UV)
214 (Shimadzu LC-2010A-HT, Shimadzu, Japan) was used according to the method described by
215 Xue *et al* and Kudo *et al* to analyse the CHX [35,36]. The analysed solutions containing CHX
216 were separated with a reverse-phase column (C18-MG, 5 μ m, 110 Å, 250 \times 46mm,
217 Phenomenex Gemini) maintained at 40°C. The mobile phase consisted of acetonitrile/water
218 (40:60) containing 0.05% (v/v) trifluoroacetic acid, 0.05% (v/v) heptafluorobutyric acid and
219 0.1% (v/v) triethylamine. The flow-rate was 1 ml/min and the injection volume 10 μ l. CHX
220 was detected at 260 nm with a retention time of 6-7 min.

221 **2.5.2. CHX phase solubility diagram**

222 Phase solubility studies were carried out according to the method described by Higushi and
223 Connors [37]. Excess amount of CHX was added to Me β CD and Me β CD polymer (PCD)
224 solutions in water at different concentrations ranging from 0 to 80 mM in CD cavities. The
225 mixtures were shaken (120 rpm, room temperature) for 24h and filtered through a 0.45 μ m
226 membrane filter. The concentration of CHX in the supernatant was determined with the
227 HPLC method previously described. Phase solubility diagrams were obtained by plotting the
228 solubility of CHX in mmol/L versus CD concentration in mmol/L. According to [38],
229 association constant (K_a) value of CD/CHX inclusion complex was calculated from the slope
230 of the linear part of the phase-solubility diagrams using the following equation:

231 Eq. 5:

$$232 K_a = \text{Slope} / (S_0 * (1 - \text{Slope}))$$

233 Where S_0 is the intrinsic solubility of **CHX** in the absence of CD and *Slope* is the slope of **the**
234 **linear part** of the phase–solubility profile.

235 The solubilizing **power** of CD was evaluated by the complexation efficiency (CE)
236 parameter. CE is the complex to free CD concentrations ratio and was calculated from the
237 slope of the phase solubility diagram:

238 **Eq. 6:**

$$239 \quad CE = S_0 * K_a = [CD-CHX] / [CD] = Slope / (1-Slope)$$

240 Where [CD-**CHX**] is the concentration of dissolved inclusion complex and [CD] is the
241 concentration of free CD.

242 **2.5.3. CHX loading and release kinetics**

243 **Drug Loading** - Textile samples (\varnothing 11mm) were impregnated in a saturated aqueous
244 suspension of **CHX** (0.4 mg/mL) under stirring (210 rpm) overnight at room temperature. The
245 samples were briefly rinsed with ultrapure water, dried and stored at 37°C before evaluation.

246 **Sorption capacities of textiles** were measured by immersion of samples (\varnothing 11 mm) in 15 ml
247 of NaOH (0.5 M) under sonication for 1 hour and then under stirring (300 rpm) for 24 hours.
248 The **pH** of supernatant solutions (n=6) **were** adjusted to 4 with acetic acid (50% (v/v)) and
249 **CHX** was quantified by HPLC.

250 **CHX release kinetic** - Loaded samples (\varnothing 11mm) were placed in 24 well-plate (CytoOne®)
251 containing 1 mL of PBS solution under 80 rpm at 37°C. At predetermined **intervals** (30
252 minutes – 37 days), the release medium was completely removed and **replaced** with fresh
253 PBS. The **CHX** content in the release medium (n=6) was determined by HPLC. Release
254 medium and sample were stored at 37°C for microbiological evaluation.

255 **2.5.4. *In vitro* microbiological evaluation**

256 Microbiological tests were performed according to the standardized Kirby–Bauer method
257 [39]. 50 µL of the release medium were placed in wells in Mueller Hinton agar plates pre-
258 inoculated with *Staphylococcus aureus* (*S. aureus*, CIP224) strains. After 24 h of incubation
259 (37°C), the inhibition zone was measured. The values were plotted as a function of the
260 soaking time in PBS to evaluate the antimicrobial activity of the disk sample and release
261 medium (n=6)

262

263 3. Results and discussion

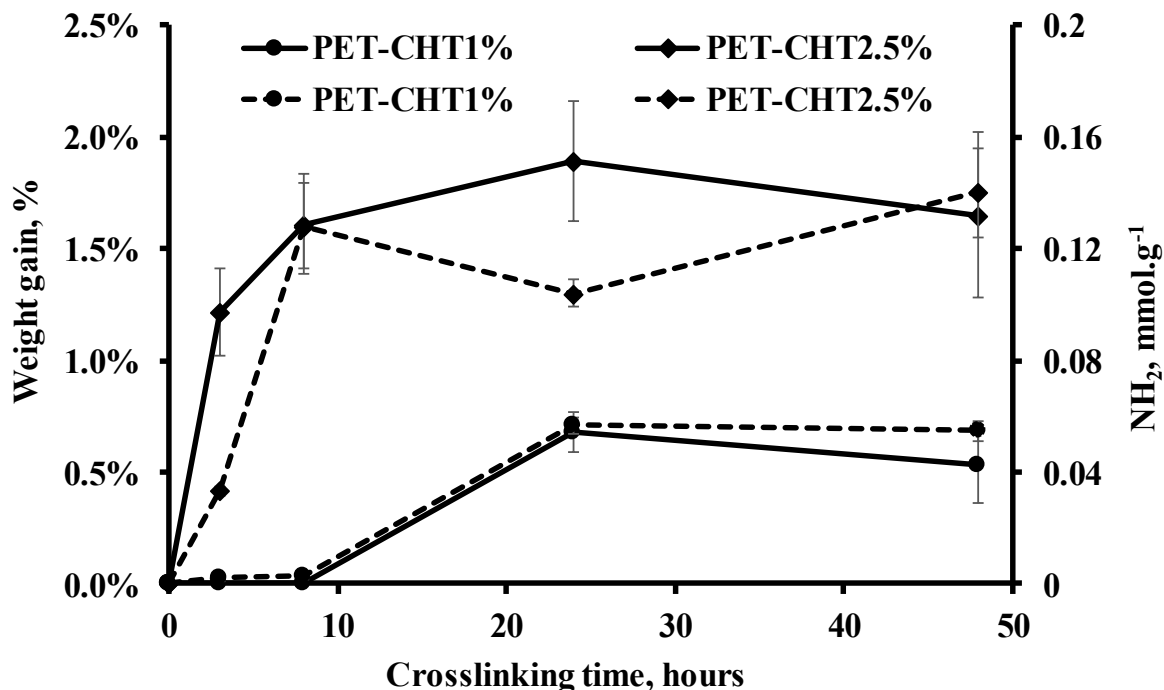
264 3.1. PET modification with CHT-Gpn

265 3.1.1. Influence of CHT concentration and reaction time

266 CHT immobilization on PET through crosslinking reaction with Gpn could be observed
267 thanks to parallel weight gain and amino groups assessments after washing samples with
268 diluted acetic acid. Figure 2 shows the parallel evolution of the weight gain and the amino
269 groups content on the textile in function of the time of crosslinking for PET samples
270 impregnated and roll-padded in CHT solutions (1.0% and 2.5% (w/v)) containing Gpn at
271 concentration fixed to 0.1% w/v. For the highest concentration of CHT (2.5% (w/v)), the
272 weight gain and the amount of amino groups rapidly increased and reached a plateau value at
273 24 hours with a maximum of 1.9%-wt and 0.15 mmol.g⁻¹ respectively. For the lower
274 concentration of CHT (1% (w/v)), the crosslinking reaction could be detected by both
275 characterization techniques only from 8 hours of reaction. A maximum value was reached
276 after 24 hours, with a weight gain and amino content of 0.68%_w and 0.06 mmol.g⁻¹
277 respectively. For both parameters, the degree of functionalization was 2.8 times higher in
278 2.5%w/v compared to 1%w/v CHT solutions, so that a linear response was observed. CHT
279 crosslinking reaction by Gpn is produced by the nucleophilic substitution of the ester function
280 of Gpn by the primary amine group of CHT to form a secondary amide and also by the
281 nucleophilic attack on the dihydropyran group of Gpn by the primary amine of CHT resulting
282 in the formation of a six membered nitrogen heterocycle [26]. Besides, the self-
283 polymerization of Gpn forming chromophore groups absorbing at 605 nm induced the
284 progressive blue dyeing of the textiles. This observation is in accordance with the different
285 studies on the crosslinking evaluation of CHT by Gpn both in term of reaction time (24 hours)
286 than in the blue coloration in studies dealing with CHT hydrogels [40], matrices [41] or
287 nanofibers [19] crosslinked by Gpn. According to the reaction kinetic study, we opted for

288 applying a CHT concentration of 2.5% (w/v) for 24 hours as optimal conditions to obtain a
289 maximum and repeatable yield of functionalization on the textiles.

290



291

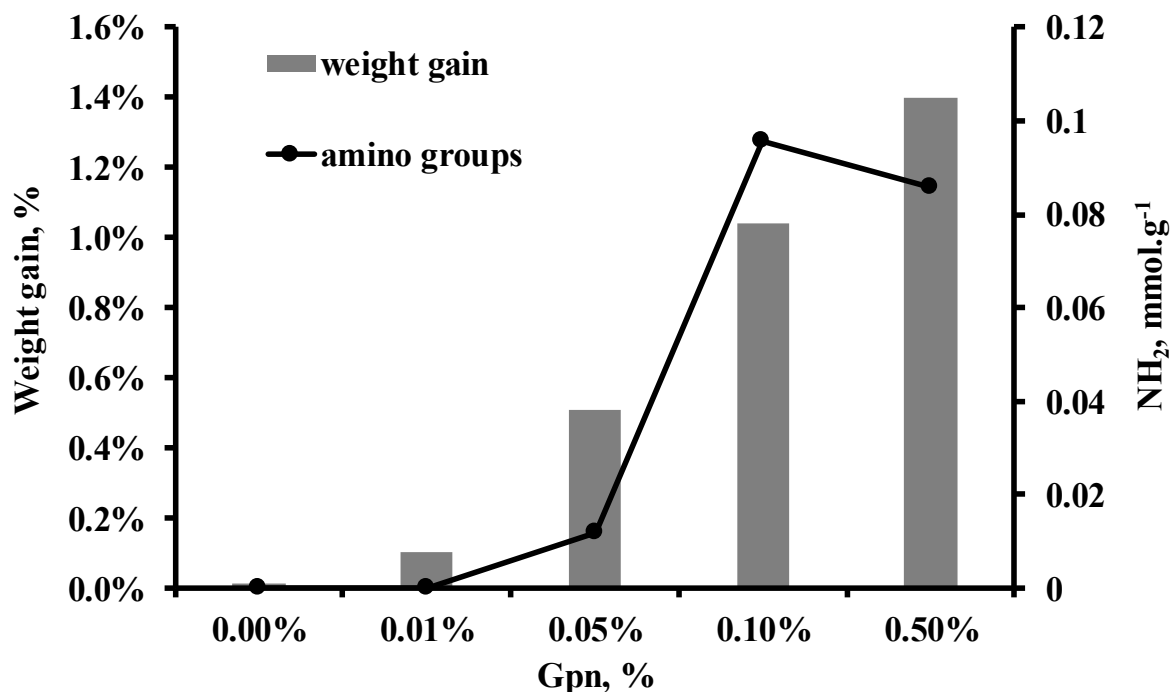
292 *Figure 2: Weight gain (solid line) and of the amino groups (-NH₂) (dashed line) contents in*
293 *mmol/g of the PET textile functionalized with CHT (concentrations 1% and 2.5% (w/v))*
294 *reticulated with Gpn (concentration 0.1% (w/v)) in function of the reaction time at 25°C.*

295 **3.1.2. Influence of the concentration of Gpn**

296 Samples were impregnated in CHT solutions whose concentration was fixed to
297 2.5% w/v) and Gpn in variable concentrations from 0.01 up to 0.5% w/v, roll-padded and left
298 in the humid ambience at 25°C for 24 hours. Figure 3 shows that the weight gain increased
299 from 0.2%-wt up to 1.4%-wt when Gpn increased from 0.05 to 0.1% w/v. It is worth
300 mentioning that in absence of Gpn, CHT was completely removed during the washing step.
301 The amount of amino groups determined by spectrophotometry increased with the Gpn
302 concentrations and reached an optimal value (0.1 mmol/g) for Gpn concentration of 0.1%

303 (w/v). Besides, the blue dyeing of the textile significantly appeared after the 24 hours period
304 of exposure in moist ambience at Gpn concentration higher than 0.1% (w/v). Despite their
305 highest weight increase, samples reticulated in presence of 0.5% w/v Gpn displayed amino
306 groups content in the same range of order as those prepared from 0.1% Gpn. This was
307 probably due to a surface saturation phenomenon that involved the stabilization of the surface
308 density of amino groups accessible to acid orange dye.

309 According to these results, we opted for applying a Gpn concentration of 0.1% (w/v) as
310 the best compromise with regard to the resulting weight gain (1.0% wt) and amino groups
311 density (0.1 mmol/g) on the PET-CHT supports. This support called PET-CHT presented a
312 cationic surface (after protonation of CHT amino groups) that was used for the build-up of the
313 PEM system as described in the next section.

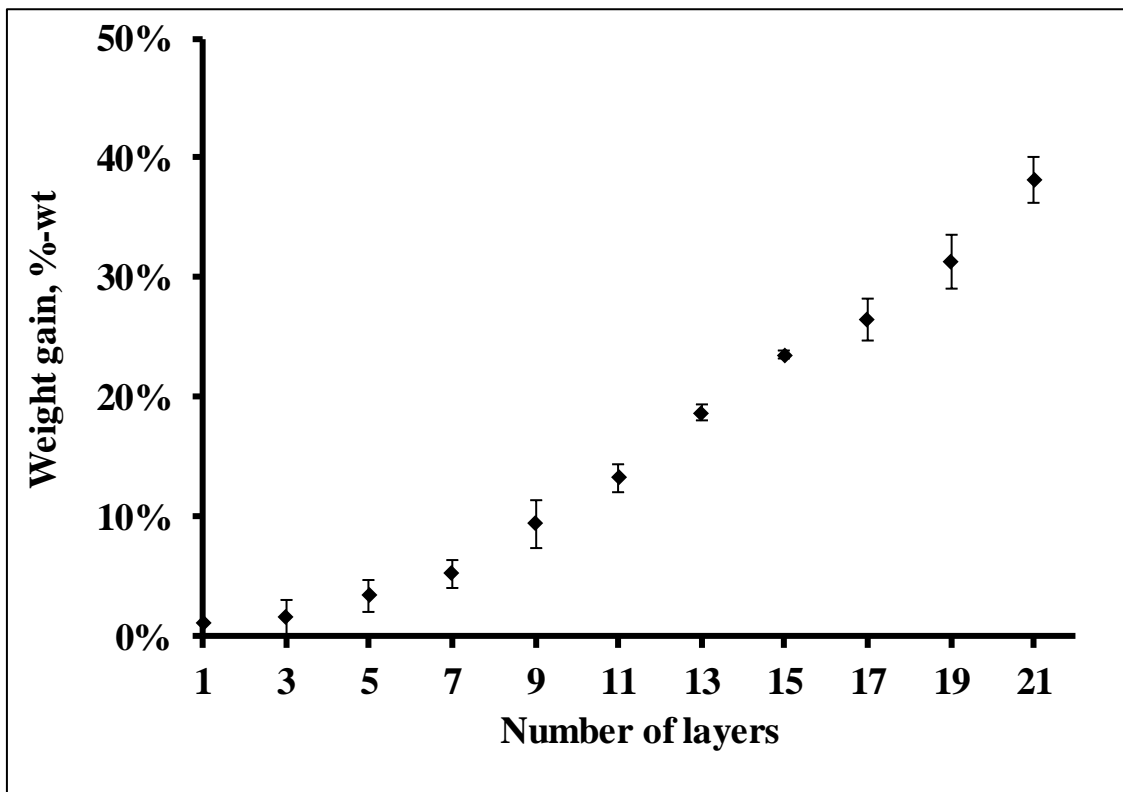


314

315 *Figure 3: Influence of the concentration of the crosslinking agent (Gpn, 25°C, 24 hours) on*
316 *the weight gain and on amino groups content (mmol/g) of the PET textile. The concentration*
317 *of CHT was fixed to 2.5% (w/v) and the reaction time was 24 hours.*

318 **3.2. Build-up of the polyelectrolyte multilayer system (PEM) on PET-CHT**

319 Figure 4 reports the weight gain of PET samples after the preliminary CHT
320 immobilization with **Gpn** (PET-CHT sample) and in the course of the subsequent cycles of
321 the dip-coating process. The polyelectrolyte complex formation through electrostatic
322 interactions between ammonium groups of CHT crosslinked by **Gpn** on PET-CHT surface
323 (layer #1) and the carboxylate groups of the water-soluble anionic CD polymer occurred and
324 induced the first **PCD** layer deposition (layer #2). By a phenomenon of charge
325 overcompensation, the surface acquired an anionic charge available for the self-assembly of
326 the next CHT layer (layer #3) and this was repeated in order to build-up a LbL coating made
327 of up to 21 layers.



328
329 *Figure 4: Weight gain (in %-wt) of the PET textile with the number of CHT layers. Layer#1*
330 *corresponds to the CHT layer reticulated with **Gpn**. The following odd numbered layers*
331 *correspond to self-assembled CHT layers alternately deposited with **PCD** layers. **PCD** and*
332 *CHT concentrations used in the dip coating process were 0.3%w/v and 0.5% w/v respectively*

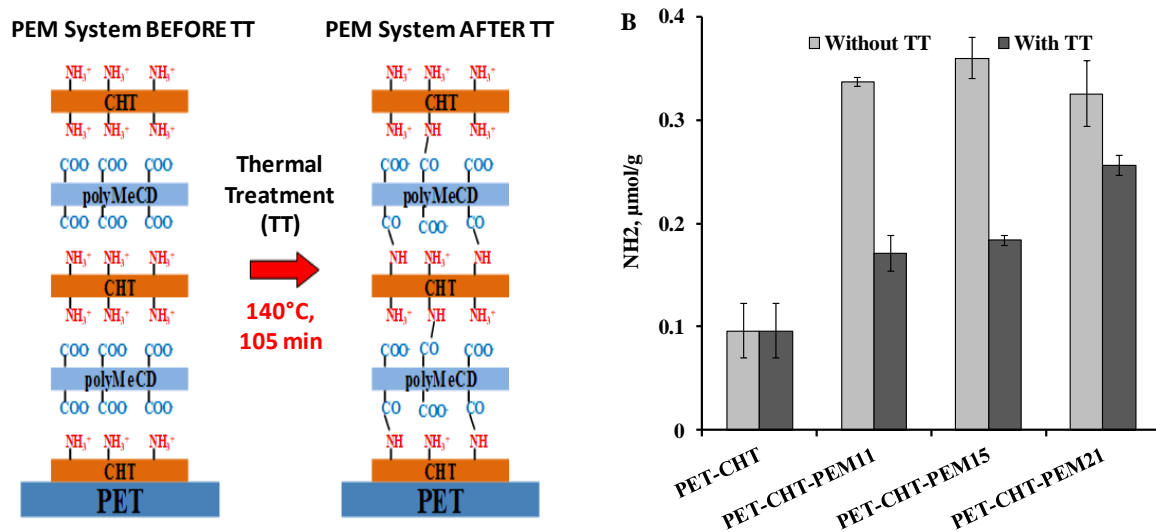
333 As observed in **Figure 4**, the growth profile of the LbL assembled multilayer consists of an
334 exponential followed by a linear part that is classically reported in similar studies. In the
335 present case, the transition between both exponential and linear regimes (called the *switch*
336 *point*) [42] occurs after the fifth CHT layer deposition (3.37% wt) and then a linear evolution
337 of the weight gain reached up to 38.13% wt (21 layers) ($r^2 = 0.9943$). The exponential part can
338 be explained by the coalescence of initially formed islands of polyelectrolytes on the fibres
339 surface that progressively leads to homogeneous coating. Once the available surface is
340 covered and if polyelectrolytes are not able to diffuse into the multilayer system, a linear
341 growth of the film is then observed [43–46].

342 **3.2.1. PEM stabilization by heat post-treatment**

343 Once dipped in saline solutions, PEM assemblies present more or less rapid degradation due
344 to the dissociation of the polyelectrolyte complexes involved by the competing ionic species
345 from the solution. ~~Such phenomenon is currently reported in the literature, and in our previous~~
346 ~~works. For example, Martin et al (2013b) [30] displayed degradation in PBS buffer at pH 7.4~~
347 ~~within 4 days of a similar PEM system based on CHT and PCD.~~ To circumvent this, we
348 previously successfully applied ~~a thermal treatment at 140°C to a similar PEM system based~~
349 ~~on CHT and PCD [30] on the one hand, and on CHT-PCD based nanofibers on the other hand~~
350 ~~[47]. Such strategy was recently successfully applied by our group on electrospun nanofibers~~
351 ~~based on CHT and PCD polyelectrolyte complexes. As a matter of fact, we could observe that~~
352 ~~a thermal treatment at 140°C markedly improved the stability of nanofibers over a period of~~
353 ~~two weeks in pH5.5 buffered solution while nanofibers without thermal treatment were~~
354 ~~readily solubilized in such acidic medium.~~ We could evidence that such thermal post
355 **treatment** provoked the crosslinking of the polyelectrolyte complex through amide groups
356 **formation** from carboxylic groups of **PCD** and amino groups of CHT [47] ~~as displayed in~~
357 ~~figure 5A.~~

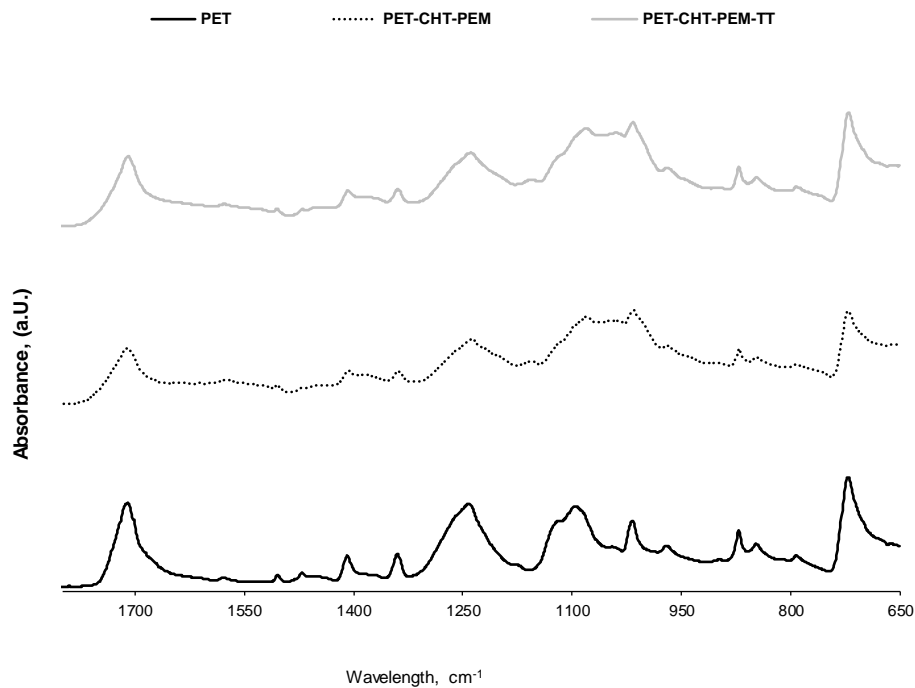
358 ~~Therefore, applying the same strategy to the PEM coating was expected to provide the same~~
 359 ~~crosslinking reaction between CHT and PCD layers as schematized in Figure 5A. This~~
 360 ~~crosslinking reaction was~~ confirmed by titrating the amino functions on PET-CHT-PEMn
 361 samples before and after the thermal post-treatment (TT) (Figure 5B). Indeed, before the
 362 thermal treatment, the density of amino functions considerably increased after PEM build-up
 363 [325 to 350 nmol.g⁻¹] compared to PET-CHT [95.8 nmol.g⁻¹]. Unlike what was observed for
 364 the PET-CHT sample, the thermal treatment of samples modified with the LbL film provoked
 365 a significant decrease of amino functions. This confirmed our hypothesis of the partial
 366 conversion of both some amino groups of CHT layers and some carboxylic acid groups of CD
 367 layers into amide bonds resulting in the stabilization of the LbL assembly.

368 It is worth mentioning that a ATR-FTIR study was carried out in order to evidence 1) LbL
 369 build-up on the PET support, and 2) the formation of amide groups induced by thermal post-
 370 treatment. However as displayed in supplementary data (Figure S1), except a new band
 371 corresponding to C-O-C vibration in polysaccharides at 1038 cm⁻¹ appearing on spectra of
 372 treated samples, the fingerprint of PET masked most of the expected signals due to LbL
 373 deposition.



374

375 *Figure 5: (A) Scheme of the formation of amide bond within the PEM system during heat*
376 *treatment (140°C - 1h45). (B) Amino groups content of PET textiles modified with CHT*
377 *crosslinked with Gpn and coated with PEM films based on 11, 15 and 21 CHT layers before*
378 *and after thermal post treatment (TT) at 140°C during 105 min.*
379

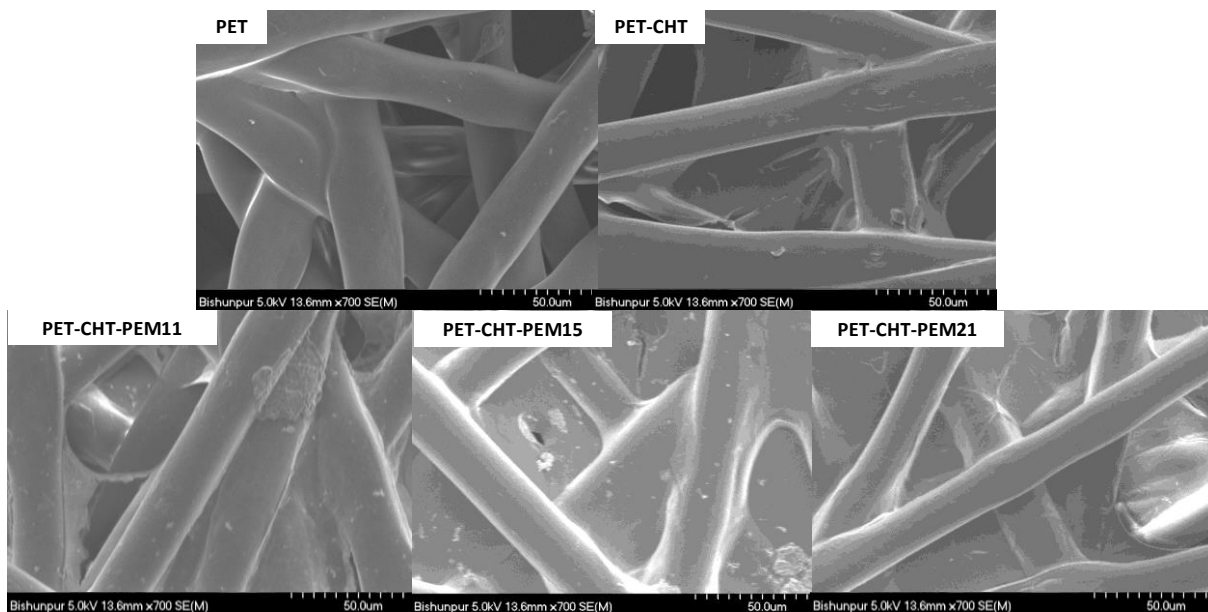


380
381
382 **Figure S1: FTIR spectra for the different stage of functionalisation, i.e. PET, PET with**
383 **multilayer system (PET-CHT-PEM) and PET with multi-Layer System (PET-CHT-PEM-TT).**
384

385 **3.3. Scanning Electron Microscopy**

386 Textile surfaces at different stages of their conception were analyzed by scanning electron
387 microscopy (Figure 6). The virgin PET fibres are smooth, spaces between fibers form open
388 pores, and some fibres are slightly deformed or welded due to the textile manufacturing
389 process by heat setting. PET-CHT reveals the presence of CHT visible especially at the
390 crossings of the fibres, but does not appear obviously due to the spreading of CHT coating
391 forming a thin film corresponding to 1.0% of the total weight of the material at this step of the

392 process. When the multilayer system is applied, the coverage of the textile fibres by the PEM
393 coating can be clearly observed, as well as the pores close-up. Despite the fibers coating and
394 porosity filling by CHT-PCD polyelectrolyte complex, only a moderate stiffening of the
395 treated textiles was noticed, even in case of PEM 21 sample.

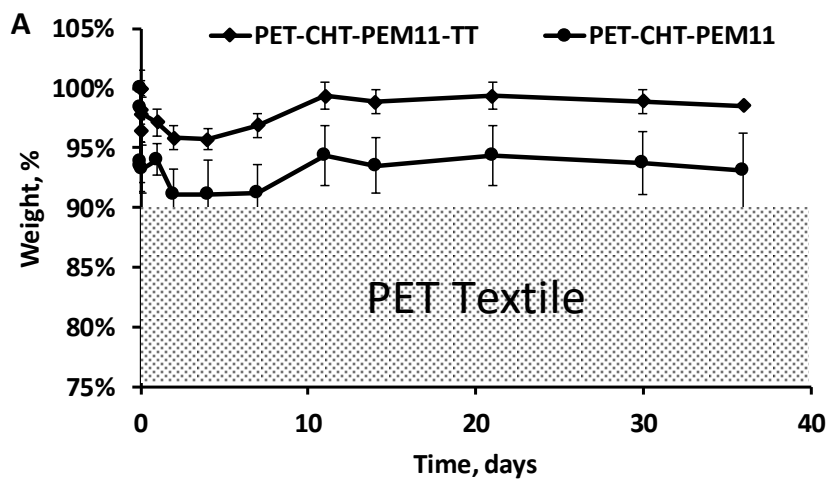


396
397 Figure 6: SEM micrographs obtained by scanning electron microscopy of samples at
398 different stages of the process, virgin PET, PET modified by Gnp crosslinked CHT, and after
399 PEM deposition up to 11, 15 and 21 CHT layers.

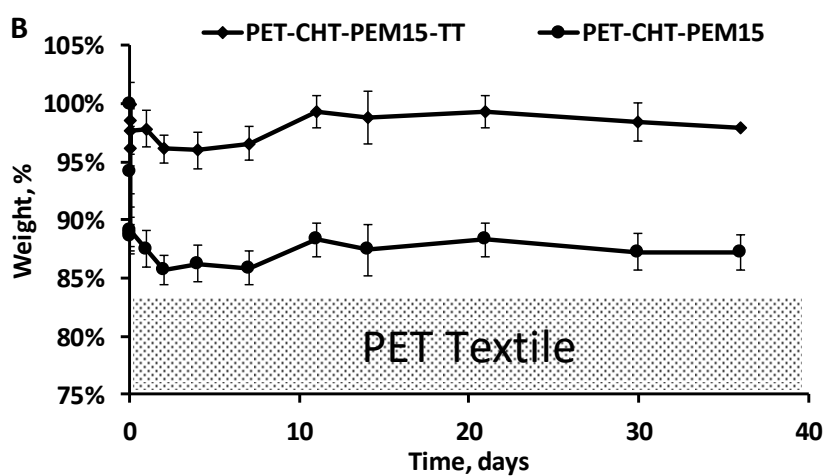
400 3.4. *In vitro* degradation studies

401 Figure 7 shows the evolution of the weight of the multilayer system as a function of the
402 degradation time in PBS medium. No significant degradation was observed for PET- CHT
403 samples after 5 weeks in PBS, confirming the stability of the first layer of CHT immobilized
404 on PET by crosslinking with Gpn. On the other hand, PEM self-assembled systems without
405 thermal post treatment revealed a rapid and significant degradation after 3 days in the PBS
406 solution. Thus, PEM11; PEM15 and PEM21 lost 10%, 15% and 20% of their initial weights
407 respectively, corresponding to the totality of the PEM coating for each of the samples.
408 Conversely, heat-treated PEM systems displayed degradations values inferior to 5%. This

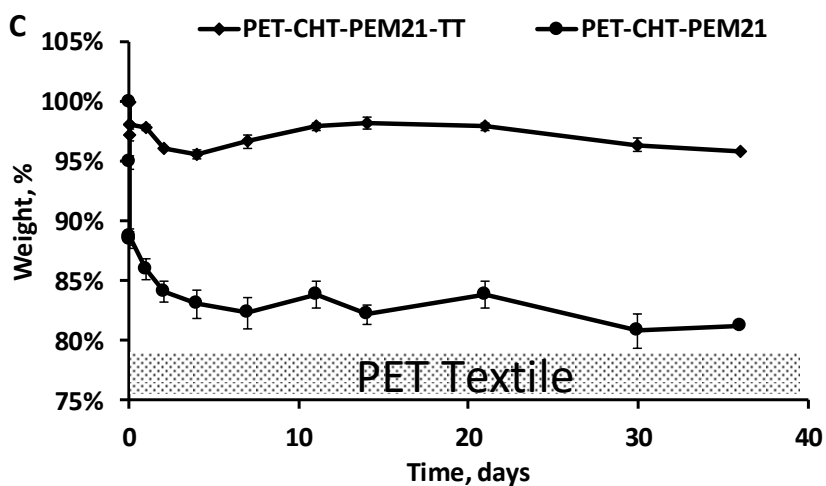
409 result confirms is an indirect evidence of the crosslinking of the LbL coating upon heating as
410 discussed previously.



411



412



413

414 *Figure 7: Weight (%w) of the PEMn samples (n= 11; 15; 21) systems with or without thermal*
 415 *treatment (TT) in function of the time of degradation in PBS (37°C, 80 rpm)..*

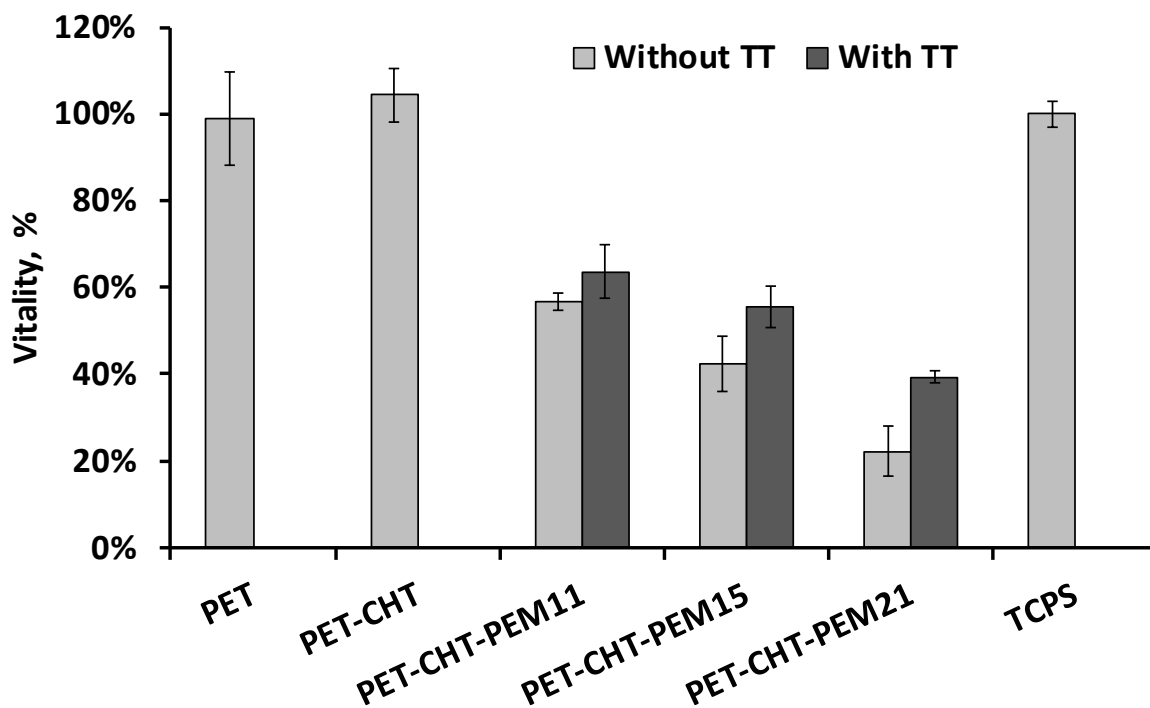
416

417 **3.5. *In vitro* biological evaluation**

418 The cytocompatibility of the textiles was evaluated with epithelial cells line L132 (ATTC-
419 CCL5), for their high sensibility with toxic products according to ISO 10993-5. Cells were
420 seeded onto the different textiles: PET, PET- CHT-**Gpn**, PEMn samples with or without TT.

421 Figure 8 confirms the cytocompatibility of PET support which remained unchanged after
422 coating with crosslinked CHT by **Gpn**, 99.0% and 104.4% respectively, after 3 days of
423 incubation. This result is in agreement with the work of Li et al. and Lau et al. who showed
424 the good cytocompatibility of electrospun CHT membranes crosslinked with **Gpn** in contact
425 with purified Schwann cells and fibroblasts (L929) [19,48].

426 Nevertheless, **Figure 8** also displays that samples coated with PEM provoked a decrease
427 of cell vitality when increasing the number of layers from PEM15 to PEM21. Besides, in a
428 former study from our group, Martin et al (2013b) [30] observed the same phenomenon
429 explained by the release of **PCD** in the culture medium that provoked the pH decrease and cell
430 death. Our results display that heat treatment applied to PEM samples improved their
431 cytocompatibility due to crosslinking reactions between **PCD** and CHT that prevented the
432 above mentioned phenomena. Furthermore, the lower cell proliferation on PEM system
433 compared to PET-CHT can also be explained by a low initial adhesion of the cells on the
434 coating surface. Indeed, Muzzio et al also showed that cell adhesion decreased when thermal
435 treatment was applied to the multilayer system [49].



437

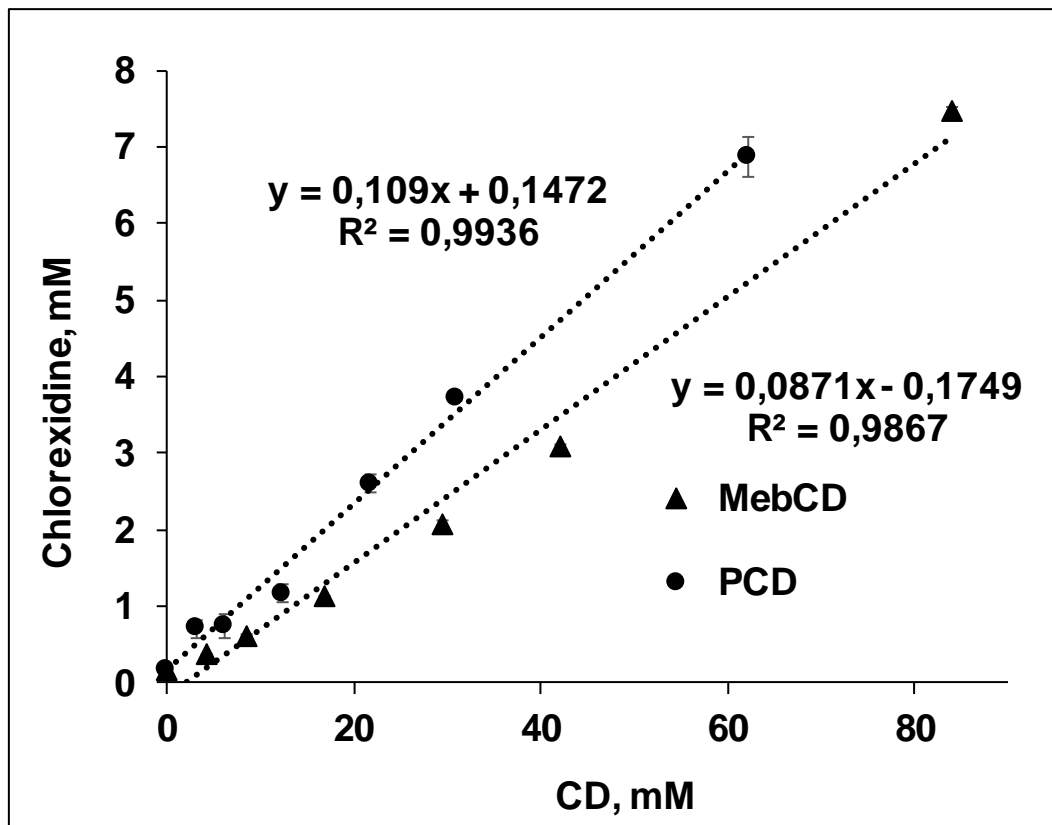
438 Figure 8 : Cell vitality (Alamar Blue method) of L132 cells on PET, PET-CHT and PET-
 439 CHT-PEM_n samples (n = 11; 15; 21) with or without thermal post treatment (140°C, 1:45h)
 440 after 3 days of culture (37°C, 5% CO₂, 100% RH), without renewal of the culture medium
 441 (n=6).

442 3.6. Drug sorption and Drug release

443 3.6.1. Solubility Diagram of CHX

444 Solubility enhancement studies of CHX in presence of Me β CD and Me β CD polymer
 445 (PCD) were carried out using the phase solubility method (Figure 9). CHX solubility linearly
 446 increased with Me β CD ($r^2=0.987$) and PCD ($r^2=0.994$) concentration, displaying in all cases
 447 AL-type profiles. Inclusion complexes of CHX with Me β CD and PCD[50] were evidenced by
 448 an association constant respectively of 640 M⁻¹ and 820 M⁻¹. S₀ of CHX in water at room
 449 temperature was = 0.15 mM \pm 0.015 mM while a maximum of 6.87 mM \pm 0.25 mM was
 450 obtained in presence of 62.1 mM of PCD. So PCD increased remarkably the solubility of

451 **CHX** by a factor 50. This result can be explained by the crosslinked macromolecular structure
452 of **PCD** interacting with the aromatic groups of CHX through *host-guest* interactions with
453 neighboring CD **cavities on the one hand, and through ionic interactions between cationic**
454 **biguanidinium groups of CHX** and free carboxylate groups carried by the citrate groups
455 crosslinks [51,52].



456

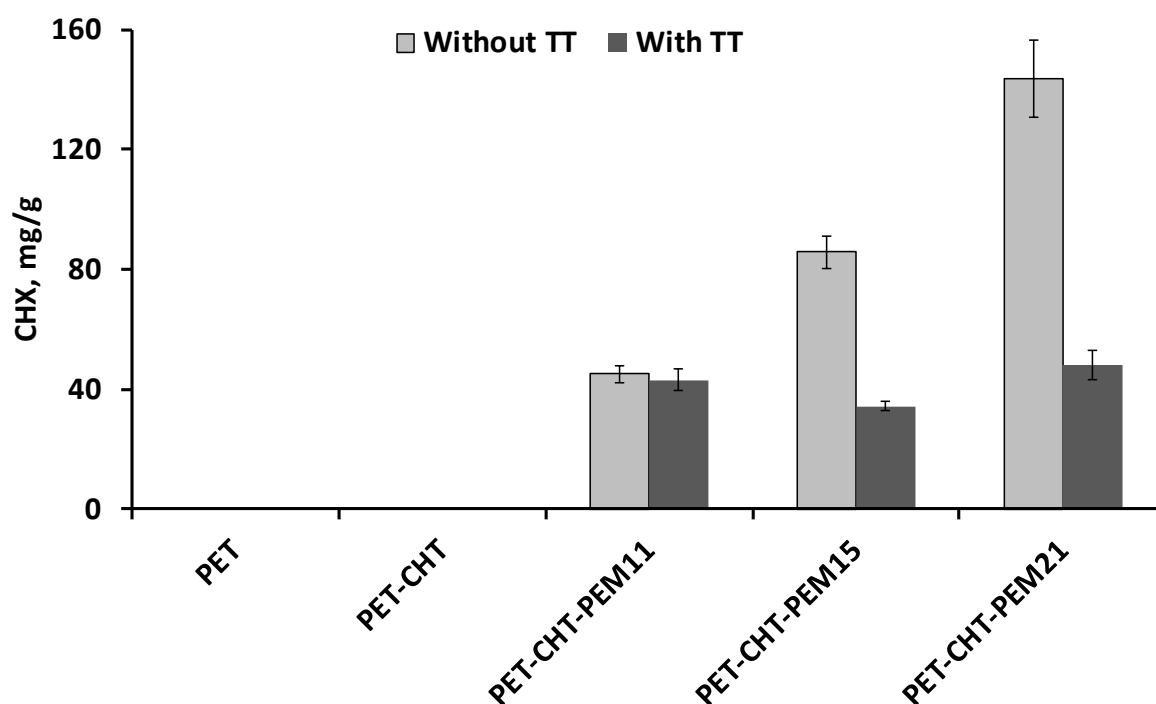
457 Figure 9: Solubility diagram of **CHX** with increasing concentrations of MeβCD and MeβCD
458 polymer (**PCD**) in aqueous solution at room temperature after 24 hours of stirring (240 rpm).
459 $S_0 = 0.15 \pm 0.015$ mmol/L at room temperature

460 3.6.2. **CHX** Loading on PEM samples

461 Textile samples were impregnated in **CHX** 0.4 mg/mL aqueous solutions (**Figure 10**). It
462 clearly appears that PEM samples could adsorb **CHX** on the contrary of virgin PET and PET-
463 CHT samples. These results highlight the crucial role played by **PCD** in the **CHX** loading. In
464 addition, increasing the number of layers in the PEM system emphasizes this phenomenon.

465 Thus, the amount of adsorbed CHX increased with the number of layers from 45.1 mg/g
466 (PEM11) up to 143.7 mg/g (PEM21). However, PEM samples after heat treatment displayed
467 reduced CHX uptakes compared to untreated ones. Furthermore, CHX uptake in this case was
468 no related to the number of layers. This can be explained by the crosslinking of the PEM,
469 which limits its swelling, and therefore CHX diffusion into the LbL coating. Elsewhere,
470 Diamanti et al. (2016) [53] have shown that a heat treatment applied to a multilayer system
471 reduced significantly the wettability of the surface (water contact angle 36° vs 95° with TT
472 (145°C))

473



474

475 Figure 10 : CHX adsorbed onto PET, PET-CHT and PET-CHT-PEM_n samples (n= 11; 15;
476 21) with or without thermal treatment. Textile samples are impregnated in CHX solution (0.4
477 mg/ml) overnight. Loaded textiles are desorbed in NaOH solution (0.5M, 4 hours).

478 3.6.3. *CHX release from PEM samples*

479 Interestingly, **Figure 12A** shows that the number of layers applied to the textile has an
480 impact on i) the percentage of **CHX** immediately released (Burst effect), ii) the percentage of
481 **CHX** delivered over time and iii) the release time.

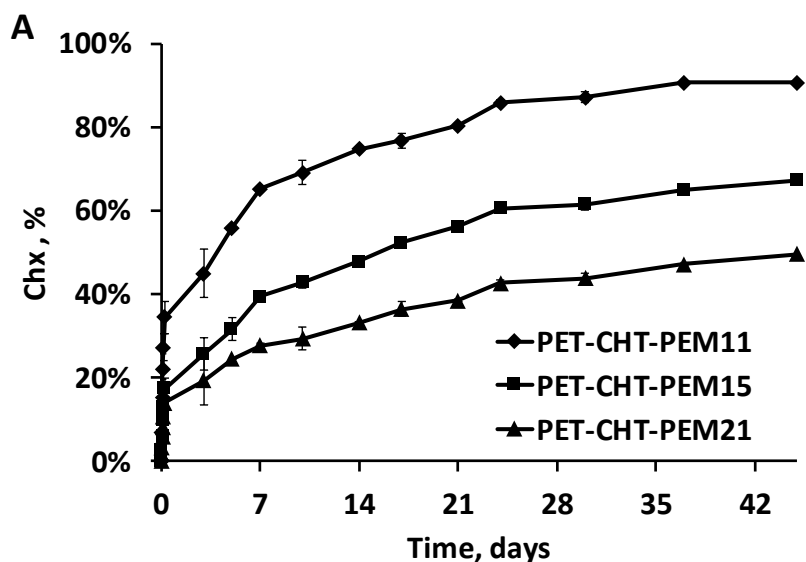
482 As a matter of fact, **Figure 11** displays the sudden release of **CHX** from all PEM samples
483 within the first instants of the release test. The extension of this burst release was related to
484 the number of layers in orders PEM11> PEM15>PEM21, corresponding to 34%, 17%, 13%,
485 and 47%, 24% and 8% before and after thermal treatment respectively. This fast release step
486 can be explained by the liberation of **CHX** in interaction with the LbL coating through weak
487 and non-specific interactions with the polyelectrolytes (hydrogen and electrostatic bondings).
488 After the burst release, delayed release of **CHX** was observed in a second phase where the
489 influence of thermal treatment on the release profile is observed. As a matter of fact, in case
490 of PEM samples without thermal treatment the decreasing of slope of the curves against time
491 of release reveals that the delivered dose decreased with time up to 45 days. On contrary,
492 concerning thermally treated samples, an almost linear release profile was observed, synonym
493 of a constant rate of delivery within the whole period of the experiment.

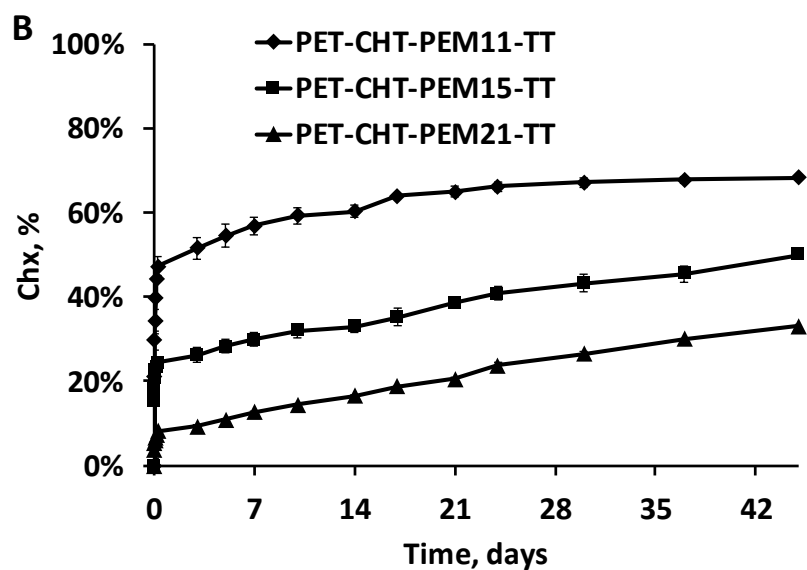
494 Finally, **Figure 11** also displays the influence of the number of layers on the overall
495 released **CHX** dose within the 45 days period for samples before (**Figure 11A**) and after
496 (**Figure 11B**) thermal treatment. As a matter of fact, after 45 days, 91, 67 and 50% of loaded
497 **CHX** were released from PEM11, PEM15 and PEM21, respectively and these values
498 decreased down to 68, 50 and 33% after thermal treatment.

499 In conclusion, the release of **CHX** could be controlled not only by the number of layers
500 but also by the application of a thermal treatment. Firstly, the number of layers controls
501 coating thickness in the PEM system. If thickness increases, the percentage of drug released
502 decrease and the release is prolonged. In relation to **Figure 7**, the release is initially controlled

503 by degradation phenomenon resulting in a burst effect, then by a diffusion / degradation
504 phenomenon with the remaining layers of polyelectrolytes on the textile. Secondly, the release
505 is also controlled by the inclusion of CHX inside the cavities of CDs as shown on cellulose
506 functionalized with CDs [51,54].

507 Thirdly, as observed in Figure 12B, the release profile is also controlled by the
508 crosslinking of the PEM system upon heat treatment. Interestingly, the thermal treatment
509 contributed to slow down the release rate of the CHX in function of the number of layers
510 applied to the textile. Indeed, after 45 days, the PET-CHT-PEM21 system released 40% of the
511 CHX while the thermal-treated system released only 25%.





513

514 Figure 11. In batch CHX release in PBS (pH 7.4, 80 rpm, 37°C) from PET-CHT-PEMn
 515 samples (n = 11; 15; 21) without (A) and with (B) thermal treatment (total medium renewal at
 516 each time point). Textile samples were preliminarily impregnated in CHX solution (0.4
 517 mg/ml) overnight.

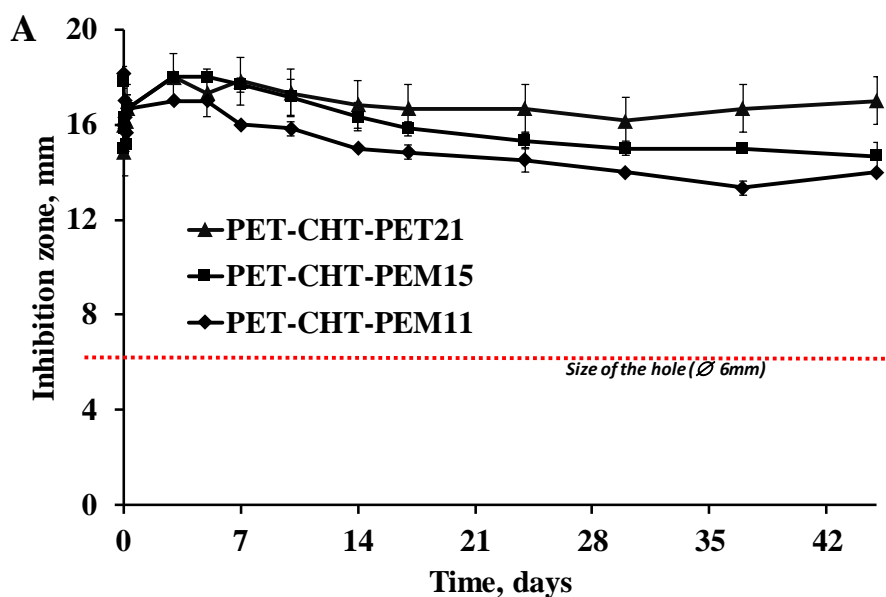
518 3.6.4. Antibacterial activity

519 The antibacterial effect against *S. aureus* of aliquots withdrawn from release medium (PBS
 520 (pH 7.4, 37°C, 80 rpm) is plotted against time in Figure 12. The inhibition zone size varied
 521 with the contact time, the number of self-assembled layers applied on the textile, and with the
 522 application of the thermal treatment. Firstly, an overview of Figure 12 revealed that the
 523 antibacterial activity of the release media persisted along the 45 days period of the assay.
 524 Nevertheless, Figure 12A shows the diameter of the zone of inhibition is increased with the
 525 number of layers applied on the textile in relation to the release profile obtained in Figure 11.
 526 Indeed, the amount of CHX release increased with the number of layers. Figure 12B also
 527 shows the impact of the number of layers on antibacterial activity. Interestingly, whatever the
 528 release time and the number of layers, the diameter of the zone of inhibition is lower than that
 529 observed for the same textiles without thermal treatment. This also confirmed the results

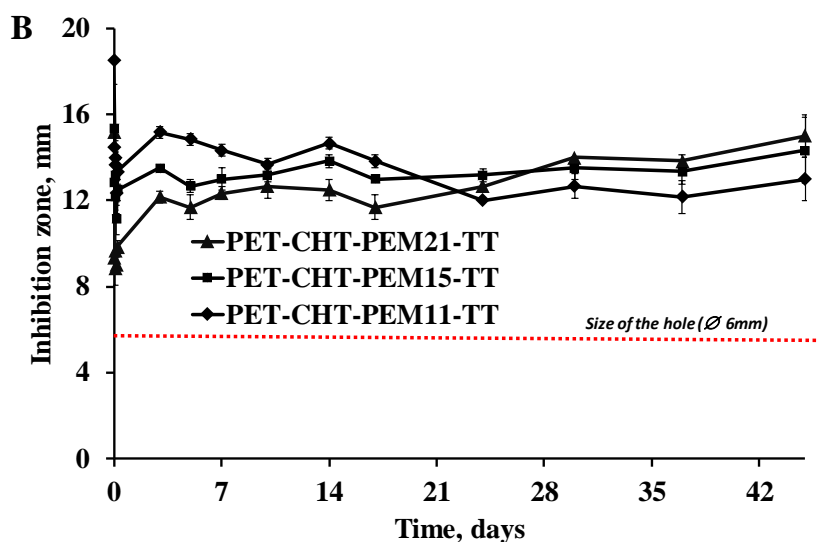
530 obtained in terms of release. Indeed, the amount of CHX released is lower for thermally
531 treated textiles compared to untreated ones. Finally, the number of layers applied to the textile
532 and the thermal post treatment could control the release of the CHX while having antibacterial
533 activity until 45 days.

534

535



536



537

538 Figure 12. Evolution of the antimicrobial activity against *S. aureus* of release medium from
 539 PET-CHT-PEMn with or without thermal treatment in PBS (pH 7.4, 80 rpm, 37°C) with total
 540 renewal medium at each time. Textile sample are impregnated in CHX solution (0.4 mg/ml)
 541 overnight.

542 4. Conclusion

543 In this paper, we report the surface modification of a polyester nonwoven textile with CHT
 544 crosslinked in mild conditions using Gpn. The resulting surface cationic charge density was
 545 controlled by the reaction time and the concentration of the reagents (CHT and Gpn). A

546 textile treatment with a 2.5% CHT solution cross-linked with 0.1% Gpn for 24 hours seems to
547 be a good compromise to obtain an optimal amino function density for the construction of a
548 PEM system while cytocompatibility was of the support was preserved.

549 Then, a layer-by-layer coating based on PCD and CHT was built-up resulting in the enhanced
550 reservoir capacity and sustained release of CHX depending of the number of layers.
551 Nevertheless, a rapid degradation of the multilayer system has been observed. In a very
552 interesting way, a compromise was found by applying a thermal post-treatment to stabilize the
553 multilayer system and to control the release of the drug over several weeks. Despite this
554 thermal treatment reduced the drug loading capacity (especially for the highest number of
555 layers) it allowed to maintain eventhough an antibacterial activity up to 7 weeks. Furthermore,
556 thermal post-treatment also enhanced the cytoamptibility of the PEM system. In addition,
557 the antibacterial activity *in vitro* over several weeks has been demonstrated on two strains (E.
558 coli and S. aureus). *In vivo* tests still have to be performed in a next future in order to display
559 the efficiency of such modified textiles as wound dressings, and open the way to other types
560 of biomedical textiles for the prevention of infections.

561 **Acknowledgment**

562 This research was funded by FONDECYT-CONCYTEC (grant contract number 238-2015-
563 FONDECYT)

564

565

566

567

568

- 570 [1] M.A. Fonder, G.S. Lazarus, D.A. Cowan, B. Aronson-Cook, A.R. Kohli, A.J.
571 Mamelak, Treating the chronic wound: A practical approach to the care of nonhealing wounds
572 and wound care dressings, *J. Am. Acad. Dermatol.* 58 (2008) 185–206.
573 doi:10.1016/j.jaad.2007.08.048.
574
- 575 [2] V.T.M. Le, C. Tkaczyk, S. Chau, R.L. Rao, E.C. Dip, E.P. Pereira-Franchi, L. Cheng,
576 S. Lee, H. Koelkebeck, J.J. Hilliard, X.Q. Yu, V. Datta, V. Nguyen, W. Weiss, L. Prokai, T.
577 O'Day, C.K. Stover, B.R. Sellman, B.A. Diep, Critical Role of Alpha-Toxin and Protective
578 Effects of Its Neutralization by a Human Antibody in Acute Bacterial Skin and Skin Structure
579 Infections, *Antimicrob. Agents Chemother.* 60 (2016) 5640–5648. doi:10.1128/AAC.00710-
580 16.
- 581 [3] Z. Song, H. Sun, Y. Yang, H. Jing, L. Yang, Y. Tong, C. Wei, Z. Wang, Q. Zou, H.
582 Zeng, Enhanced efficacy and anti-biofilm activity of novel nanoemulsions against skin burn
583 wound multi-drug resistant MRSA infections, *Nanomedicine Nanotechnol. Biol. Med.* 12
584 (2016) 1543–1555. doi:10.1016/j.nano.2016.01.015.
585
- 586 [4] Y. Gao, R. Cranston, Recent Advances in Antimicrobial Treatments of Textiles, *Text.*
587 *Res. J.* 78 (2008) 60–72. doi:10.1177/0040517507082332.
- 588 [5] P. Gupta, S. Chhibber, K. Harjai, Efficacy of purified lactonase and ciprofloxacin in
589 preventing systemic spread of *Pseudomonas aeruginosa* in murine burn wound model, *Burns*
590 *J. Int. Soc. Burn Inj.* 41 (2015) 153–162. doi:10.1016/j.burns.2014.06.009.
591
- 592 [6] A.K. Gupta, P. Batra, P. Mathur, A. Karoung, B.T. Thanbuana, S. Thomas, M.
593 Balamurugan, J. Gunjiyal, M.C. Misra, Microbial epidemiology and antimicrobial
594 susceptibility profile of wound infections in out-patients at a level 1 trauma centre, *J. Patient*
595 *Saf. Infect. Control.* 3 (2015) 126–129. doi:10.1016/j.jpsic.2015.06.001.
596
- 597 [7] J.M. Schierholz, J. Beuth, Implant infections: a haven for opportunistic bacteria, *J.*
598 *Hosp. Infect.* 49 (2001) 87–93. doi:10.1053/jhin.2001.1052.
599
- 600 [8] K.K. Chung, J.F. Schumacher, E.M. Sampson, R.A. Burne, P.J. Antonelli, A.B.
601 Brennan, Impact of engineered surface microtopography on biofilm formation of
602 *Staphylococcus aureus*, *Biointerphases.* 2 (2007) 89–94. doi:10.1116/1.2751405.
603
- 604 [9] P.H.S. Kwakman, A.A. te Velde, C.M.J.E. Vandenbroucke-Grauls, S.J.H. van
605 Deventer, S.A.J. Zaat, Treatment and prevention of *Staphylococcus epidermidis* experimental
606 biomaterial-associated infection by bactericidal peptide 2, *Antimicrob. Agents Chemother.* 50
607 (2006) 3977–3983. doi:10.1128/AAC.00575-06.
608
- 609 [10] B.S. Nagoba, B.J. Wadher, A.K. Rao, G.D. Kore, A.V. Gomashe, A.B. Ingle,
610 A simple and effective approach for the treatment of chronic wound infections caused by
611 multiple antibiotic resistant *Escherichia coli*, *J. Hosp. Infect.* 69 (2008) 177–180.

612 doi:10.1016/j.jhin.2008.03.014.

613

614 [11] M. van de Lagemaat, A. Grotenhuis, B. van de Belt-Gritter, S. Roest, T.J.A.
615 Loontjens, H.J. Busscher, H.C. van der Mei, Y. Ren, Comparison of methods to evaluate
616 bacterial contact-killing materials, *Acta Biomater.* 59 (2017) 139–147.
617 doi:10.1016/j.actbio.2017.06.042.

618

619 [12] V. Ambrogi, D. Pietrella, M. Nocchetti, S. Casagrande, V. Moretti, S. De
620 Marco, M. Ricci, Montmorillonite–chitosan–chlorhexidine composite films with antibiofilm
621 activity and improved cytotoxicity for wound dressing, *J. Colloid Interface Sci.* 491 (2017)
622 265–272. doi:10.1016/j.jcis.2016.12.058.

623

624 [13] S.S.D. Kumar, N.K. Rajendran, N.N. Houreld, H. Abrahamse, Recent advances
625 on silver nanoparticle and biopolymer-based biomaterials for wound healing applications, *Int.*
626 *J. Biol. Macromol.* 115 (2018) 165–175. doi:10.1016/j.ijbiomac.2018.04.003.

627

628 [14] J. Berger, M. Reist, J.M. Mayer, O. Felt, R. Gurny, Structure and interactions
629 in chitosan hydrogels formed by complexation or aggregation for biomedical applications,
630 *Eur. J. Pharm. Biopharm.* 57 (2004) 35–52. doi:10.1016/S0939-6411(03)00160-7.

631

632 [15] F.L. Mi, Y.C. Tan, H.C. Liang, R.N. Huang, H.W. Sung, In vitro evaluation of
633 a chitosan membrane cross-linked with genipin, *J. Biomater. Sci. Polym. Ed.* 12 (2001) 835–
634 850.

635

636 [16] X.F. Liu, Y.L. Guan, D.Z. Yang, Z. Li, K.D. Yao, Antibacterial action of
637 chitosan and carboxymethylated chitosan, *J. Appl. Polym. Sci.* 79 (2001) 1324–1335.
638 doi:10.1002/1097-4628(20010214)79:7<1324::AID-APP210>3.0.CO;2-L.

639

640 [17] H.K. No, N. Young Park, S. Ho Lee, S.P. Meyers, Antibacterial activity of
641 chitosans and chitosan oligomers with different molecular weights, *Int. J. Food Microbiol.* 74
642 (2002) 65–72. doi:10.1016/S0168-1605(01)00717-6.

643

644 [18] H. Liu, Y. Du, X. Wang, L. Sun, Chitosan kills bacteria through cell membrane
645 damage, *Int. J. Food Microbiol.* 95 (2004) 147–155. doi:10.1016/j.ijfoodmicro.2004.01.022.

646

647 [19] Q. Li, X. Wang, X. Lou, H. Yuan, H. Tu, B. Li, Y. Zhang, Genipin-crosslinked
648 electrospun chitosan nanofibers: Determination of crosslinking conditions and evaluation of
649 cytocompatibility, *Carbohydr. Polym.* 130 (2015) 166–174.
650 doi:10.1016/j.carbpol.2015.05.039.

651

652 [20] H. Tanuma, T. Saito, K. Nishikawa, T. Dong, K. Yazawa, Y. Inoue,
653 Preparation and characterization of PEG-cross-linked chitosan hydrogel films with
654 controllable swelling and enzymatic degradation behavior, *Carbohydr. Polym.* 80 (2010) 260–
655 265. doi:10.1016/j.carbpol.2009.11.022.

656
657
658
659
660
661
662
663
664
665
666
667
668
669
670
671
672
673
674
675
676
677
678
679
680
681
682
683
684
685
686
687
688
689
690
691
692
693
694
695
696
697
698
699

[21] F.-L. Mi, Y.-C. Tan, H.-F. Liang, H.-W. Sung, In vivo biocompatibility and degradability of a novel injectable-chitosan-based implant, *Biomaterials*. 23 (2002) 181–191.

[22] M. Rinaudo, New way to crosslink chitosan in aqueous solution, *Eur. Polym. J.* 46 (2010) 1537–1544. doi:10.1016/j.eurpolymj.2010.04.012.

[23] M. Zhang, X.H. Li, Y.D. Gong, N.M. Zhao, X.F. Zhang, Properties and biocompatibility of chitosan films modified by blending with PEG, *Biomaterials*. 23 (2002) 2641–2648. doi:10.1016/S0142-9612(01)00403-3.

[24] F. Aubert-Viard, A. Martin, F. Chai, C. Neut, N. Tabary, B. Martel, Nicolas Blanchemain, Chitosan finishing nonwoven textiles loaded with silver and iodide for antibacterial wound dressing applications, *Biomed. Mater.* 10 (2015) 015023.

[25] R.A.A. Muzzarelli, Genipin-crosslinked chitosan hydrogels as biomedical and pharmaceutical aids, *Carbohydr. Polym.* 77 (2009) 1–9. doi:10.1016/j.carbpol.2009.01.016.

[26] M.F. Butler, Y.-F. Ng, P.D.A. Pudney, Mechanism and kinetics of the crosslinking reaction between biopolymers containing primary amine groups and genipin, *J. Polym. Sci. Part Polym. Chem.* 41 (2003) 3941–3953. doi:10.1002/pola.10960.

[27] F.-L. Mi, S.-S. Shyu, C.-K. Peng, Characterization of ring-opening polymerization of genipin and pH-dependent cross-linking reactions between chitosan and genipin, *J. Polym. Sci. Part Polym. Chem.* 43 (2005) 1985–2000. doi:10.1002/pola.20669.

[28] B.. Liu, T.. Huang, A novel wound dressing composed of nonwoven fabric coated with chitosan and herbal extract membrane for wound healing., *Polym. Compos.* 31 (2010) 1037–1046.

[29] A. Martin, N. Tabary, L. Leclercq, J. Junthip, S. Degoutin, F. Aubert-Viard, F. Cazaux, J. Lyskawa, L. Janus, M. Bria, B. Martel, Multilayered textile coating based on a β -cyclodextrin polyelectrolyte for the controlled release of drugs, *Carbohydr. Polym.* 93 (2013) 718–730. doi:10.1016/j.carbpol.2012.12.055.

[30] A. Martin, N. Tabary, F. Chai, L. Leclercq, J. Junthip, F. Aubert-Viard, C. Neut, M. Weltrowski, N. Blanchemain, B. Martel, Build-up of an antimicrobial multilayer coating on a textile support based on a methylene blue-poly(cyclodextrin) complex, *Biomed. Mater. Bristol Engl.* 8 (2013) 065006. doi:10.1088/1748-6041/8/6/065006.

[31] B. Martel, D. Ruffin, M. Weltrowski, Y. Lekchiri, M. Morcellet, Water-soluble polymers and gels from the polycondensation between cyclodextrins and poly(carboxylic acid)s: A study of the preparation parameters, *J. Appl. Polym. Sci.* 97 (2005) 433–442. doi:10.1002/app.21391.

[32] G. McDonnell, A.D. Russell, Antiseptics and disinfectants: activity, action, and

700 resistance, *Clin. Microbiol. Rev.* 12 (1999) 147–179.

701

702 [33] J. Langgartner, H.-J. Linde, N. Lehn, M. Reng, J. Schölmerich, T. Glück,
703 Combined skin disinfection with chlorhexidine/propanol and aqueous povidone-iodine
704 reduces bacterial colonisation of central venous catheters, *Intensive Care Med.* 30 (2004)
705 1081–1088. doi:10.1007/s00134-004-2282-9.

706

707 [34] M. Weltrowski, M. Morcellet, B. Martel, Cyclodextrin polymers and/or
708 cyclodextrin derivatives with complexing properties and ion-exchange properties and method
709 for the production thereof, US6660804B1, 2003.
710 <https://patents.google.com/patent/US6660804B1/en> (accessed August 27, 2018).

711

712 [35] Y. Xue, M. Tang, Y. Hieda, J. Fujihara, K. Takayama, H. Takatsuka, H.
713 Takeshita, High-performance liquid chromatographic determination of chlorhexidine in whole
714 blood by solid-phase extraction and kinetics following an intravenous infusion in rats, *J. Anal.*
715 *Toxicol.* 33 (2009) 85–91.

716

717 [36] K. Kudo, N. Ikeda, A. Kiyoshima, Y. Hino, N. Nishida, N. Inoue,
718 Toxicological analysis of chlorhexidine in human serum using HPLC on a polymer-coated
719 ODS column, *J. Anal. Toxicol.* 26 (2002) 119–122.

720

721 [37] T. Higuchi, K. Connors, *Advances in Analytical Chemistry and*
722 *Instrumentation.*, *Adv. Anal. Chem. Instrum.* (1965) 117–212.

723

724 [38] M.E. Brewster, T. Loftsson, Cyclodextrins as pharmaceutical solubilizers, *Adv.*
725 *Drug Deliv. Rev.* 59 (2007) 645–666. doi:10.1016/j.addr.2007.05.012.

726

727 [39] G. Vermet, S. Degoutin, F. Chai, M. Maton, C. Flores, C. Neut, P.E. Danjou,
728 B. Martel, N. Blanchemain, Cyclodextrin modified PLLA parietal reinforcement implant with
729 prolonged antibacterial activity, *Acta Biomater.* 53 (2017) 222–232.
730 doi:10.1016/j.actbio.2017.02.017.

731

732 [40] L. Gao, H. Gan, Z. Meng, R. Gu, Z. Wu, X. Zhu, W. Sun, J. Li, Y. Zheng, T.
733 Sun, G. Dou, Evaluation of genipin-crosslinked chitosan hydrogels as a potential carrier for
734 silver sulfadiazine nanocrystals, *Colloids Surf. B Biointerfaces.* 148 (2016) 343–353.
735 doi:10.1016/j.colsurfb.2016.06.016.

736

737 [41] M.P. Klein, C.R. Hackenhaar, A.S.G. Lorenzoni, R.C. Rodrigues, T.M.H.
738 Costa, J.L. Ninow, P.F. Hertz, Chitosan crosslinked with genipin as support matrix for
739 application in food process: Support characterization and β -d-galactosidase immobilization,
740 *Carbohydr. Polym.* 137 (2016) 184–190. doi:10.1016/j.carbpol.2015.10.069.

741

742 [42] A.S. Vikulina, Y.G. Anissimov, P. Singh, V.Z. Prokopović, K. Uhlig, M.S.
743 Jaeger, R. von Klitzing, C. Duschl, D. Volodkin, Temperature effect on the build-up of

744 exponentially growing polyelectrolyte multilayers. An exponential-to-linear transition point,
745 *Phys. Chem. Chem. Phys.* 18 (2016) 7866–7874. doi:10.1039/C6CP00345A.

746

747 [43] L. Richert, P. Lavalle, E. Payan, X.Z. Shu, G.D. Prestwich, J.-F. Stoltz, P.
748 Schaaf, J.-C. Voegel, C. Picart, Layer by Layer Buildup of Polysaccharide Films: Physical
749 Chemistry and Cellular Adhesion Aspects, *Langmuir*. 20 (2004) 448–458.
750 doi:10.1021/la035415n.

751

752 [44] B. Seantier, A. Deratani, Polyelectrolytes at Interfaces: Applications and
753 Transport Properties of Polyelectrolyte Multilayers in Membranes, in: *Ion. Interact. Nat.*
754 *Synth. Macromol.*, Wiley-Blackwell, 2012: pp. 683–726. doi:10.1002/9781118165850.ch18.

755

756 [45] G. Ladam, P. Schaad, J.C. Voegel, P. Schaaf, G. Decher, F. Cuisinier, In Situ
757 Determination of the Structural Properties of Initially Deposited Polyelectrolyte Multilayers,
758 *Langmuir*. 16 (2000) 1249–1255. doi:10.1021/la990650k.

759

760 [46] F. Caruso, D.N. Furlong, K. Ariga, I. Ichinose, T. Kunitake, Characterization
761 of Polyelectrolyte–Protein Multilayer Films by Atomic Force Microscopy, Scanning Electron
762 Microscopy, and Fourier Transform Infrared Reflection–Absorption Spectroscopy, *Langmuir*.
763 14 (1998) 4559–4565. doi:10.1021/la971288h.

764

765 [47] S. Ouerghemmi, S. Degoutin, N. Tabary, F. Cazaux, M. Maton, V. Gaucher, L.
766 Janus, C. Neut, F. Chai, N. Blanchemain, B. Martel, Triclosan loaded electrospun nanofibers
767 based on a cyclodextrin polymer and chitosan polyelectrolyte complex, *Int. J. Pharm.* 513
768 (2016) 483–495. doi:10.1016/j.ijpharm.2016.09.060.

769

770 [48] Y.-T. Lau, L.-F. Kwok, K.-W. Tam, Y.-S. Chan, D.K.-Y. Shum, G.K.-H. Shea,
771 Genipin-treated chitosan nanofibers as a novel scaffold for nerve guidance channel design,
772 *Colloids Surf. B Biointerfaces*. 162 (2018) 126–134. doi:10.1016/j.colsurfb.2017.11.061.

773

774 [49] N.E. Muzzio, M.A. Pasquale, E. Diamanti, D. Gregurec, M.M. Moro, O.
775 Azzaroni, S.E. Moya, Enhanced antiadhesive properties of chitosan/hyaluronic acid
776 polyelectrolyte multilayers driven by thermal annealing: Low adherence for mammalian cells
777 and selective decrease in adhesion for Gram-positive bacteria, *Mater. Sci. Eng. C Mater. Biol.*
778 *Appl.* 80 (2017) 677–687. doi:10.1016/j.msec.2017.07.016.

779

780 [50] P. Saokham, C. Muankaew, P. Jansook, T. Loftsson, Solubility of
781 Cyclodextrins and Drug/Cyclodextrin Complexes, *Mol. Basel Switz.* 23 (2018).
782 doi:10.3390/molecules23051161.

783

784 [51] N. Tabary, F. Chai, N. Blanchemain, C. Neut, L. Pauchet, S. Bertini, E.
785 Delcourt-Debruyne, H.F. Hildebrand, B. Martel, A chlorhexidine-loaded biodegradable
786 cellulosic device for periodontal pockets treatment, *Acta Biomater.* 10 (2014) 318–329.
787 doi:10.1016/j.actbio.2013.09.032.

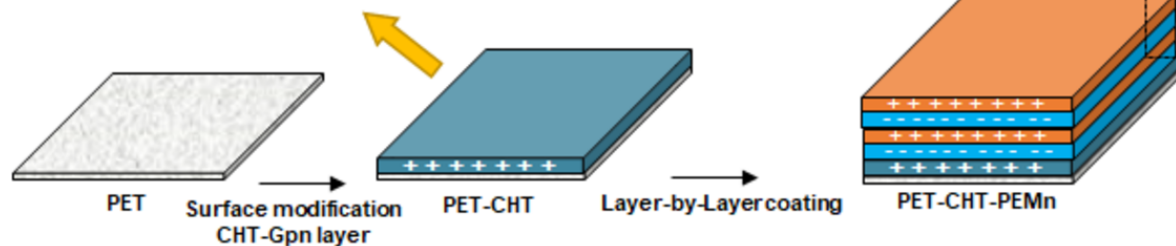
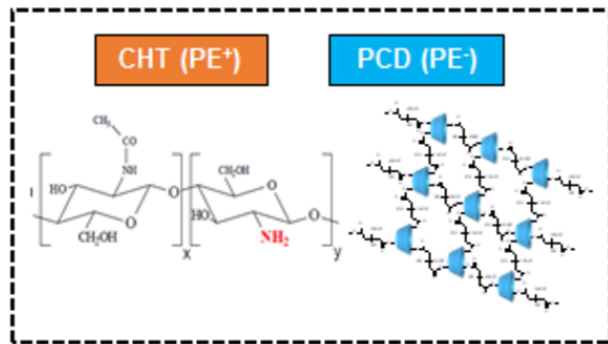
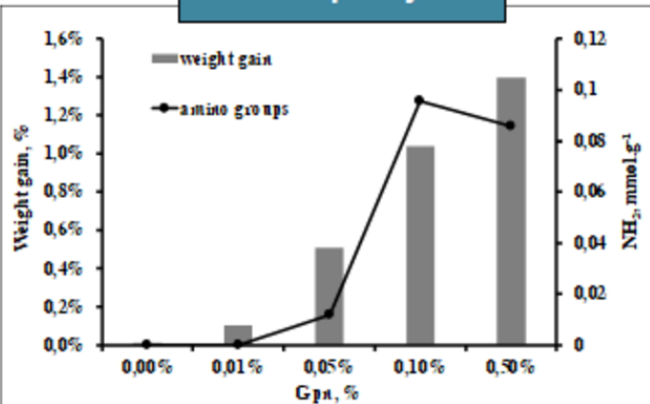
788
789
790
791
792
793
794
795
796
797
798
799
800
801
802

[52] J. Junthip, N. Tabary, F. Chai, L. Leclercq, M. Maton, F. Cazaux, C. Neut, L. Paccou, Y. Guinet, J.-N. Staelens, M. Bria, D. Landy, A. Hédoux, N. Blanchemain, B. Martel, Layer-by-layer coating of textile with two oppositely charged cyclodextrin polyelectrolytes for extended drug delivery, *J. Biomed. Mater. Res. A.* 104 (2016) 1408–1424. doi:10.1002/jbm.a.35674.

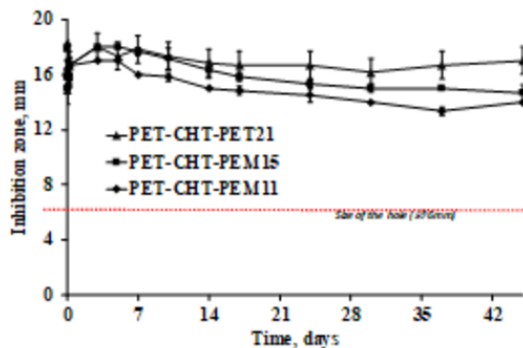
[53] E. Diamanti, N. Muzzio, D. Gregurec, J. Irigoyen, M. Pasquale, O. Azzaroni, M. Brinkmann, S.E. Moya, Impact of thermal annealing on wettability and antifouling characteristics of alginate poly-l-lysine polyelectrolyte multilayer films, *Colloids Surf. B Biointerfaces.* 145 (2016) 328–337. doi:10.1016/j.colsurfb.2016.05.013.

[54] N. Lavoine, N. Tabary, I. Desloges, B. Martel, J. Bras, Controlled release of chlorhexidine digluconate using β -cyclodextrin and microfibrillated cellulose, *Colloids Surf. B Biointerfaces.* 121 (2014) 196–205. doi:10.1016/j.colsurfb.2014.06.021.

CHT-Gpn layer



Control release of CHX



Antibacterial activity against *S. aureus*

